RESEARCH ARTICLE | DECEMBER 09 2024

On the compatibility of the Madrid-2019 force field for electrolytes with the TIP4P/Ice water model ⊘

Special Collection: Molecular Dynamics, Methods and Applications 60 Years after Rahman

Samuel Blazquez (ID) ; Lucia F. Sedano (ID) ; Carlos Vega ✉ (ID)

Check for updates

View Online

Export Citation

Articles You May Be Interested In

The Madrid-2019 force field for electrolytes in water using TIP4P/2005 and scaled charges: Extension to the ions F^-, Br^-, I^-, Rb^+, and Cs^+

J. Chem. Phys. (January 2022)

Freezing point depression of salt aqueous solutions using the Madrid-2019 model

J. Chem. Phys. (April 2022)

Further extension of the Madrid-2019 force field: Parametrization of nitrate (NO_3^-) and ammonium (NH_4^+) ions
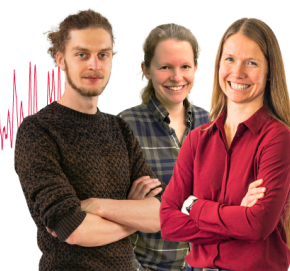
J. Chem. Phys. (December 2023)

25 August 2025 10:04:49

On the compatibility of the Madrid-2019 force field for electrolytes with the TIP4P/Ice water model

View Online   Export Citation   CrossMark

Samuel Blazquez, [ID] Lucia F. Sedano, [ID] and Carlos Vega[a] [ID]

AFFILIATIONS

Dpto. Química Física I, Fac. Ciencias Químicas, Universidad Complutense de Madrid, 28040 Madrid, Spain

Note: This paper is part of the JCP Special Topic on Molecular Dynamics, Methods and Applications 60 Years after Rahman.
[a]**Author to whom correspondence should be addressed:** cvega@quim.ucm.es

ABSTRACT

The Madrid-2019 force field was recently developed to perform simulations of electrolytes in water. The model was specifically parameterized for TIP4P/2005 water and uses scaled charges for the ions. In this work, we test the compatibility of the Madrid-2019 force field with another water model: TIP4P/Ice. We shall denote this combination as Madrid-2019(TIP4P/Ice) force field. The key idea of this combination is to keep the ion–ion (Madrid-2019) and water–water (TIP4P/Ice) interactions unaltered with respect to the original models and taking the Lennard-Jones parameters for the ion–water interactions from the Madrid-2019 force field. By implementing this approach, we have maintained a reasonably good performance of the model regarding the densities and structural features of aqueous solutions, albeit yielding a moderately higher viscosity than the original model. However, the standout achievement of this new combination lies in its effective reproduction of the absolute values of the freezing temperatures of a number of ionic aqueous solutions, which could also be useful when studying hydrate formation from a two-phase system containing an aqueous solution in contact with a gas.

I. INTRODUCTION

Water is the lifeblood of our planet, an important resource that sustains all forms of life and plays an indispensable role in natural processes. Water exists in various forms, including liquid, solid, and gaseous states, each of which serves unique purposes in our environment. While the liquid form is essential for sustaining life, the solid forms of water, such as ice and hydrates, are equally vital. The freezing of the upper layer of water protects the aquatic life by maintaining stable temperature regimes.[1,2] Ice also plays a crucial role in Earth's climate system, reflecting sunlight and influencing global temperature patterns.[2] On the other hand, hydrates are non-stoichiometric solid compounds, where water molecules are found forming a crystal lattice structure in which small molecules of gases are trapped. These compounds are of high interest for the industry as they can be used as a potential source of energy or as an alternative way to storage molecules of interest.[3] However, when we delve deeper into the complexity of water, we find another key element in this equation: salt. Over 70% of the Earth's surface is covered by salty water. Moreover, salt, in the form of dissolved ions such as sodium and chloride, is essential in human health, influencing cellular function and fluid balance.[4,5]

In this context, computer simulations play a pivotal role in advancing our understanding of water in all its forms. They enable us to grasp intricate phenomena, such as the anomalous behavior of water under extreme conditions[6–8] or the nucleation of ices[9,10] and hydrates[11,12] within a spatio-temporal realm that experimentalists cannot readily access. To accurately describe the interactions between water and salt, it is crucial to employ suitable force fields for both substances.

In the case of water potential models, the journey began in the 1980s when Jorgensen and co-workers proposed two force fields with different geometries for water: TIP3P[13] (with a negative charge in the oxygen atom) and TIP4P[13] (with a negative charge in the bisector of water). In 1987, another significant contribution emerged with the introduction of the SPC/E water model by Berendsen *et al.*[14] This model, alongside the aforementioned ones, constitutes the repertoire of water force fields that would be widely used for the next

30 years. Nonetheless, the journey did not stop there. As we entered the new millennium, improved water models appeared. Among them, we find force fields such as TIP4P-Ew,[15] TIP5P[16] (a model featuring a novel five-site geometry), TIP4P/2005,[17] and TIP4P/Ice[18] force fields. In recent years, several other promising models have emerged, including three-site models such as OPC-3[19] and TIP3P-FB,[20] as well as four-site models, such as TIP4P-FB,[20] OPC[21] or TIP4P-D.[22] In addition, there are polarizable models with computational cost several times higher compared to non-polarizable models[23] such as HBP[24] (~3 times), i-AMOEBA[25] (~5 times), BK3[26] (~10 times), or MB-Pol[27,28] (>20 times).

One can easily become overwhelmed by the multitude of water models available. Furthermore, there is not a single model able to reproduce all properties simultaneously.[29,30] Nonetheless, two widely employed models stand out due to their capability to replicate several properties. The first one is the TIP4P/2005 (which accurately describes the temperature of the maximum in density of pure water but not its freezing temperature), which is broadly use for simulating liquid and supercooled water due to its excellent performance.[6,8,31–36] The second one is TIP4P/Ice (which reproduces the freezing temperature of pure water but not the temperature of the maximum in density), which is known for providing accurate descriptions of ice polymorphs[37–39] and gas hydrates.[40–46] Thus, this model is commonly employed for nucleation or growth studies of solid phases of water.[9,47–61]

The current landscape is quite clear: to study ices, hydrates, or amorphous water, the model of choice should be TIP4P/Ice. This potential has garnered a thriving community of researchers employing it to investigate a vast range of problems. However, a challenge arises when the study involves the combination of ice and salt. In such cases, the selection of an appropriate model becomes crucial. To address this question, it is essential to delve into the available ion force fields. The most widely employed models for electrolytes have been proposed by Smith and Dang[62] and by Joung and Cheatham.[63] In addition, in recent years, a myriad of force fields tailored for salts have been developed.[62–91]

The majority of these force fields traditionally assign integer charges to ions (i.e., $\pm 1e$). However, in recent years, some authors have introduced the concept of using scaled charges for the ions to enhance the accuracy of modeling aqueous solutions and to account for polarization in a mean field approximation.[92,93] The origins of using scaled charges can be traced back to the pioneering work of Leontyev and Stuchebrukhov,[94–99] who proposed a charge of ± 0.75 for ions. Subsequently, Kann and Skinner[100] suggested that the Coulombic energy between ions at infinite dilution and infinitely large distances should be the same in experiments and in simulations. Consequently, the charge assigned to ions following this approach depends on the dielectric constant of the water model, resulting in a charge of ± 0.85 for ions in the case of the TIP4P/2005 model.

In the past few years, many authors have adopted the used of scaled charges and developed new force fields based on this idea.[92,101–116] Indeed, we have also developed a force field with charges of ± 0.85 for ions in combination with TIP4P/2005 for a variety of ions: the Madrid-2019,[91,117–119] which overtakes many traditional models in a variety of properties.[115,120–124] The increase in these new force fields with scaled charges is due to their performance in describing aqueous solutions, improving the results of traditional

unit charge models. In fact, scaled charges have been proven useful for biomolecular simulations,[125,126] describing transport properties such as viscosities[115,120] or electrical conductivities,[121] temperatures of maximum density for several salts,[127,128] the salting out effect of different gases in water,[115,122] adsorption phenomena at electrolyte solutions interfaces,[129] phase diagram of aqueous solutions of LiCl[130] or even the phase equilibrium of ice and methane hydrate in NaCl solutions.[123,124]

Due to the exceptional performance of TIP4P/Ice in describing solid phases of water and the remarkable accuracy of scaled charge models, particularly the Madrid-2019 force field, in characterizing aqueous electrolyte solutions, it is reasonable to explore the development of a new force field that combines both the TIP4P/Ice for water and the Madrid-2019 for ions. This new force field will be particularly useful to study the equilibrium between ice/hydrates and electrolyte aqueous solutions. In this study, we will present a straightforward methodology for combining these force fields, resulting in the new Madrid-2019(TIP4P/Ice) model.

II. MODEL

As previously mentioned, among the non-polarizable and rigid water models proposed in the literature, the TIP4P/2005 force field stands out as one of the most effective for studying the properties of liquid water.[17] Similarly, the Madrid-2019 force field[91,117–119] (designed in combination with water TIP4P/2005) accurately reproduces a wide range of properties of aqueous electrolyte solutions.[115,120,121,123,124,127–131] It is interesting to mention that, in general, the Madrid-2019 does not use Lorentz–Berthelot combining rules. For this reason, the Lennard-Jones (LJ) parameters of each specific interaction must be described explicitly. Although TIP4P/2005 can be regarded as a good water model, it is not perfect, and for instance, its freezing temperature is 250 K (instead of the experimental value of 273 K). This is rather inconvenient when studying ice formation from electrolyte aqueous solutions. In contrast, the melting point of TIP4P/Ice, 270 K, is much closer to the experimental value. For this reason, a significant part of the research community employs TIP4P/Ice, when performing simulation studies dealing with ice (or hydrate) formation. For this community, there is a need for a force field that allows simulations in saline environments. Therefore, we now propose a straightforward method for combining the Madrid-2019 force field with the TIP4P/Ice water model:

- For cation–cation, anion–anion, and cation–anion interactions, we use the parameters of the Madrid-2019 model (charges and LJ parameters) regardless of the water model under consideration.
- For ion–water interactions, we use the LJ parameters of the Madrid-2019 force field for both water models (TIP4P/2005 and TIP4P/Ice).

TABLE I. Force field parameters for TIP4P/2005[17] and TIP4P/Ice[18] models.

Model	$\sigma_{O_w-O_w}$ (Å)	$\varepsilon_{O_w-O_w}$ (kJ/mol)	q_H (e)	d_{OM} (Å)
TIP4P/2005	3.1589	0.774 90	0.5564	0.1546
TIP4P/Ice	3.1668	0.882 18	0.5897	0.1577

TABLE II. Lennard-Jones parameters σ_{ij} (in Å) of the Madrid-2019 force field for the ions Li^+, Na^+, K^+, Rb^+, Cs^+, Mg^{2+}, Ca^{2+}, Sr^{2+}, Ba^{2+}, NH_4^+, F^-, Cl^-, Br^-, I^-, SO_4^{2-}, and NO_3^-. O_w, O_s, and O_n are the water, sulfate, and nitrate oxygens, respectively. N_n and N_a are the nitrate and ammonium nitrogens, respectively. In cases where a numerical value is not given, we use the Lorentz–Berthelot (LB) combination rules. LB(+) indicates that the LB combining rules have been checked in binary or ternary solutions with satisfactory results. The only place where the choice of the water model enters is in bold (i.e., the LJ O_w–O_w of either the TIP4P/2005 or TIP4P/Ice water models, respectively).

	F^-	Cl^-	Br^-	I^-	Li^+	Na^+	K^+	Rb^+	Cs^+	Mg^{2+}	Ca^{2+}	Sr^{2+}	Ba^{2+}	O_w	S	O_s	N_n	O_n	N_a
F^-	3.789 82	LB	LB	LB	2.845 40	LB	3.462 50	3.572 50	3.945 50	LB	LB	LB	LB	3.774 50	LB	LB	LB	LB	3.540 00
Cl^-		4.699 06	LB	LB	2.700 00	3.005 12	3.397 00	3.996 42	4.318 54	3.000 00	3.150 00	3.300 00	3.800 00	4.238 67	LB(+)	LB(+)	LB	LB	LB(+)
Br^-			4.825 25	LB	2.614 50	3.385 00	3.798 79	3.917 25	4.334 08	2.655 19	3.670 52	3.580 00	3.900 00	4.198 50	LB	LB	LB	LB	LB(+)
I^-				5.049 75	3.204 70	3.646 58	4.005 50	4.102 88	4.437 90	2.827 07	3.941 81	3.600 00	4.200 00	4.349 50	LB	LB	LB	LB	LB
Li^+					1.439 70	LB(+)	LB	LB	LB	LB	LB(+)	LB	LB	2.120 00	LB(+)	2.844 85	LB(+)	3.300 00	LB
Na^+						2.217 37	LB(+)	LB	LB	LB(+)	LB(+)	LB	LB	2.608 38	LB(+)	LB(+)	LB(+)	3.000 00	LB
K^+							2.301 40	LB	LB	LB	LB	LB	LB	2.890 40	LB(+)	3.200 00	LB(+)	3.300 00	LB
Rb^+								2.994 98	LB	LB	LB	LB	LB	3.543 50	LB	3.4000	LB(+)	3.200 00	LB
Cs^+									3.521 013	LB	LB	LB	LB	3.662 90	LB	LB	LB(+)	3.400 00	LB
Mg^{2+}										1.162 90	LB	LB	LB	1.810 00	LB(+)	2.406 45	LB(+)	3.400 00	LB
Ca^{2+}											2.665 60	LB	LB	2.400 00	LB	LB	LB(+)	2.762 80	LB
Sr^{2+}												3.050 00	LB	2.680 00	LB	LB	LB(+)	LB(+)	LB
Ba^{2+}													3.265 60	2.968 00	LB	LB	LB(+)	3.3000	LB
O_w														**3.1589/3.1668**	LB(+)	3.404 45	LB(+)	3.230 00	3.054 00
S															3.550 00	LB	LB	LB	LB(+)
O_s																3.650 00	LB	LB	3.300 00
N_n																	3.150 00	LB(+)	3.900 00
O_n																		2.860 00	LB(+)
N_a																			3.250 00

TABLE III. Lennard-Jones parameters ε_{ij} (in kJ/mol) for the Madrid-2019 force field for the ions Li^+, Na^+, K^+, Rb^+, Cs^+, Mg^{2+}, Ca^{2+}, Sr^{2+}, Ba^{2+}, NH_4^+, F^-, Cl^-, Br^-, I^-, SO_4^{2-}, and NO_3^-, respectively. O_w, O_s, and O_n are the water, sulfate, and nitrate oxygens, respectively. N_n and N_a are the nitrate and ammonium nitrogens, respectively. In cases where a numerical value is not given, we use the Lorentz–Berthelot (LB) combination rules. LB(+) indicates that the LB combining rules have been checked in binary or ternary solutions with satisfactory results. The only place where the choice of the water model enters is in bold (i.e., the LJ O_w–O_w of either the TIP4P/2005 or TIP4P/Ice water models, respectively).

	F^-	Cl^-	Br^-	I^-	Li^+	Na^+	K^+	Rb^+	Cs^+	Mg^{2+}	Ca^{2+}	Sr^{2+}	Ba^{2+}	O_w	S	O_s	N_n	O_n	N_a
F^-	0.030 963 7	LB	LB	LB	0.110 265 5	LB	0.223 167	0.216 120 2	0.097 105	LB	LB	LB	LB	0.100 000	LB	LB	LB	LB	LB(+)
Cl^-		0.076 923	LB	LB	1.282 944	1.438 894	1.400 000	0.340 641	0.161 555 8	3.000 000	1.000 000	0.800 000	0.500 000	0.061 983	LB(+)	LB(+)	LB	LB	LB(+)
Br^-			0.112 795	LB	0.199 378	0.356 77	0.425 940	0.458 323	0.195 632	0.641 807	0.239 185	0.600 000	0.400 000	0.100 000	LB	LB	LB	LB	LB(+)
I^-				0.179 01	0.273 498	0.513 387	0.536 590	0.519 646	0.246 452	0.808 534	0.301 320	0.400 000	0.300 000	0.100 000	LB	LB	LB	LB	LB
Li^+					0.435 090	LB(+)	LB							0.700 650	LB(+)	0.803 609	LB(+)	LB(+)	LB
Na^+						1.472 356	LB(+)			LB(+)	LB(+)			0.793 388	LB(+)	LB(+)	LB(+)	LB(+)	LB
K^+							1.985 740							1.400 430	LB(+)	1.289 519	LB(+)	LB(+)	LB
Rb^+								1.862 314						0.100 000	LB	1.250 800	LB(+)	LB(+)	LB
Cs^+									0.375 959 6					0.100 000	LB(+)	2.748 743	LB(+)	LB(+)	LB
Mg^{2+}										3.651 900				12.000 000	LB	LB	LB(+)	LB(+)	LB
Ca^{2+}											0.507 200			7.250 000	LB	LB	LB(+)	LB(+)	LB
Sr^{2+}												0.455 000		4.500 000	LB	LB	LB(+)	LB(+)	LB
Ba^{2+}													0.405 000	3.400 000	LB	LB	LB(+)	0.590 000	LB
O_w														**0.774 90/0.882 180**	LB(+)	0.629 000	LB(+)	LB(+)	LB(+)
S															1.046 700	LB	LB	LB	LB(+)
O_s																0.837 400	LB	LB	LB(+)
N_n																	0.711	LB	LB(+)
O_n																		0.878	LB(+)
N_a																			0.711

25 August 2025 10:04:49

- For water–water interactions, we shall use the parameters of the TIP4P/Ice (instead of those of the TIP4P/2005) model.

In short, we only modify water–water interactions and keep the rest (ion–ion and LJ ion–water interactions) identical for both water models. It is true that there is a small difference in the Coulombic contribution of the ion–water interactions as the partial charges of the TIP4P/Ice and TIP4P/2005 models although similar are not identical. Let us stress again that in the Madrid-2019 force field, the charge of monovalent ions is $\pm 0.85e$ and that of divalent ions is $\pm 1.7e$. In the supplementary material, we provide a Gromacs *topology* file of the Madrid-2019 force field to be used with TIP4P/2005 and another one to be used with TIP4P/Ice.

With this approach, we give the reader a simple recipe to combine the TIP4P/Ice with the Madrid-2019 force field, including any combination of the following cations (Li^+, Na^+, K^+, Rb^+, Cs^+, Mg^{2+}, Ca^{2+}, Sr^{2+}, Ba^{2+}, and NH_4^+) and anions (F^-, Cl^-, Br^-, I^-, SO_4^{2-}, and NO_3^-). The LJ parameters of TIP4P/2005 and TIP4P/Ice water models are summarized in Table I. Both water models share nearly identical geometries: the same HOH angle, H–O distance, although a slightly different O–M distance. In the TIP4P/Ice model, the partial charges are slightly incremented, and so are the values of the LJ parameters (σ and ε). Therefore, it seems physically reasonable to combine the ions designed for the TIP4P/2005 model with the TIP4P/Ice model. In fact, in the recent work by Dopke *et al.*,[132] they combined ion force fields originally developed for different water models with the TIP4P/2005, observing an excellent transferability for similar water models (e.g., TIP4P-Ew[15]).

In Tables II and III, we have collected the LJ parameters of the Madrid-2019 force field. These parameters are valid regardless of the choice of the water model. Only water–water interactions would be different when choosing TIP4P/2005 or TIP4P/Ice water models (see Table I), and only the Coulombic part of the interaction between ions and water would depend on the choice of the water model as the partial charges of both water models are slightly different.

III. METHODOLOGY AND SIMULATION DETAILS

Molecular dynamics (MD) simulations have been performed using the GROMACS package[133,134] in the *NpT* and *NVT* ensembles. In all simulations, we have used the leap-frog integrator algorithm,[135] with a time step of 2 fs. For all the runs, periodic boundary conditions have been applied in all directions. We used the Nosé–Hoover thermostat[136,137] with a coupling constant of 2 ps to keep the temperature constant. For *NpT* simulations, we kept the pressure by using the Parrinello–Rahman barostat[138] also with a coupling time of 2 ps. We employed a cutoff radius of 10 Å for electrostatics and van der Waals interactions. Long-range corrections in the energy and pressure were also applied to the Lennard-Jones part of the potential. To account for the long-range electrostatic forces, we used the smooth PME method.[139] Water geometry was maintained using the LINCS algorithm.[140,141] However, in cases where we simulated the sulfate or ammonium salts, the SHAKE[142] algorithm was implemented. The reason of this change is that LINCS is faster than SHAKE, but the first one is not able to maintain the tetrahedral structure of ammonium and sulfate ions. We determined the densities through *NpT* simulations of 50 ns for a system containing 555 water molecules and the corresponding number of ions for the

desired molality (moles of solute per kilogram of water). This choice of water molecules is useful due to the fact that 10 salt molecules (10 cations and 10 anions) in 555 water molecules leads to a 1 m solution. The number of contact ion pairs (CIP) was calculated from the cation–anion radial distribution function (RDF) using the following equation:

$$n^{CIP} = 4\pi\rho_\pm \int_0^{r_{min}} g_\pm(r)\, r^2\, dr, \tag{1}$$

where $\rho_\pm$ is the lower number density after dissociation, $g_\pm$ is the cation–anion RDF, and r_{min} is the first minimum in the RDF, which must be located (when determining true CIP) at a similar distance of that of the cation-O_w RDF. It is useful to simultaneously plot the cation–anion and cation-O_w RDFs to determine if one is evaluating a CIP or a SSIP (solvent separated ion pair).

For the diffusion coefficients (D), we used a system comprised of 4440 water molecules and the corresponding number of ions and the Einstein relation,

$$D = \lim_{t\to\infty} \frac{1}{6t}\left\langle[\mathbf{r}_i(t) - \mathbf{r}_i(0)]^2\right\rangle, \tag{2}$$

where $\mathbf{r}_i(t)$ and $\mathbf{r}_i(0)$ are the position of the *i*th particle at time *t* and at a certain origin of time, respectively.

Viscosities were calculated following the work of Gonzalez and Abascal.[143] We employed the same system size as the one of the diffusion coefficients, comprised of 4440 water molecules and the corresponding number of ions. We first run a 20 ns *NpT* simulation to calculate the average volume of the system, followed by a *NVT* simulation of 50 ns. We saved the pressure tensor $P_{\alpha\beta}$ every 2 fs and used the Green–Kubo equation to calculate the viscosity,

$$\eta = \frac{V}{k_B T}\int_0^\infty \langle P_{\alpha\beta}(t_0)\, P_{\alpha\beta}(t_0 + t)\rangle_{t_0}\, dt, \tag{3}$$

where V is the volume of the system, k_B is the Boltzmann constant, T is the temperature, and $P_{\alpha\beta}$ are the non-diagonal components of the pressure tensor. The upper limit of the integral depends on the system, but usually ranges between 10 and 20 ps.

For the calculation of the freezing point depression, we employed the same methodology as in previous studies.[120,124,144,145] In particular, we put two phases into contact: a solid phase comprised of 2000 ice I_h molecules and a liquid phase containing an aqueous NaCl (KCl, $MgCl_2$) solution with a given concentration (2000 water molecules and the corresponding number of ions). The ice plane exposed at the interface was the secondary prismatic plane ($1\bar{2}10$).

IV. RESULTS

The Madrid-2019 force field[91,117–119] was designed to accurately replicate the experimental densities of the investigated salts up to their solubility limits. The emphasis on density arises from its precise measurement and well-established experimental values. Now, we shall analyze the compatibility of the Madrid-2019 when combined with the TIP4P/Ice model of water (using the strategy described in the previous section). The results obtained with the TIP4P/Ice model of water will be denoted as Madrid-2019(TIP4P/Ice), whereas the properties of the original model (with TIP4P/2005 water) will be
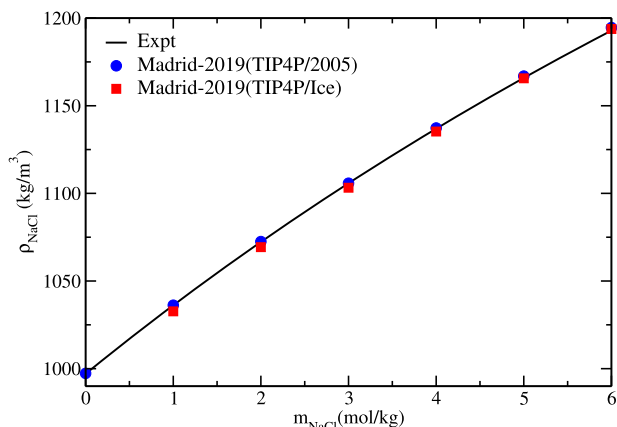
FIG. 1. Density as a function of molality at T = 298.15 K and 1 bar for NaCl aqueous solutions using the Madrid-2019(TIP4P/2005) (blue circles) and the Madrid-2019(TIP4P/Ice) (red squares) force fields. The solid black line is a fit of the experimental data taken from Ref. 146.

labeled as Madrid-2019(TIP4P/2005). All the results obtained in this work were obtained at room pressure (i.e., p = 1 bar).

A. Densities

In Fig. 1, we begin by showing the densities as a function of concentration for the Madrid-2019 model combined with both water models: Madrid-2019(TIP4P/Ice) and the original Madrid-2019(TIP4P/2005). As anticipated, the Madrid-2019(TIP4P/2005) model adeptly reproduces the densities across the entire concentration range. However, the Madrid-2019(TIP4P/Ice) model also exhibits a commendable performance, accurately emulating the experimental results. This was the expected behavior given that the Madrid-2019(TIP4P/Ice) model maintains the LJ ion–water interactions from the Madrid-2019 model while only modifying the water model. In particular, at low concentrations where water–water interactions gain significance when compared to ion–water and ion–ion interactions, the model lies slightly below the experimental trend. This discrepancy arises from the inherent characteristic of the TIP4P/Ice model, which slightly underestimates the experimental density of water at 298.15 K.

In Table IV, we provide the densities of all the salts of the Madrid-2019(TIP4P/2005) model[91,117–119] at a concentration close to the experimental solubility limit. We also include in the table the number of CIP and the difference ($\Delta\rho$) between the densities of the aqueous solutions (ρ_{salt}) and the density of pure water (ρ_{water}) for each model defined in the following equation:

$$\Delta\rho = \rho_{salt} - \rho_{water}. \quad (4)$$

It is evident that the combination of the Madrid-2019 model with the TIP4P/Ice model results, in general, in a slightly smaller value of CIP. This happens as a consequence of the slightly higher charges of the TIP4P/Ice water potential, which leads to strengthened Coulombic interactions between the water and the ions. Regarding the densities, the reported values of the Madrid-2019(TIP4P/Ice) model exhibit small deviations from those of the Madrid-2019(TIP4P/2005). $\Delta\rho$ values reveal similar trends for both

models. In summary, these findings suggest that, for the salts considered, the Madrid-2019(TIP4P/Ice) model closely aligns with the Madrid-2019(TIP4P/2005) results and, consequently, remains in close agreement with the experimental trends.

To confirm this, we have shown in Fig. 2 the difference between the $\Delta\rho$ [see Eq. (4)] obtained for the Madrid-2019(TIP4P/2005) model and the $\Delta\rho$ obtained with the Madrid-2019(TIP4P/Ice) model. We then normalized this difference by the respective concentration of each salt, typically corresponding to a value close to the experimental solubility limit. Ideally, if there were no discrepancies, the plotted values should all be 0. However, we observe some variations both above and below 0, indicating that the models' performance is not identical. Nevertheless, these deviations are relatively minor, confirming that Madrid-2019(TIP4P/Ice) effectively reproduces densities and successfully keeps under control the number of CIP of the modeled ions. Most of the salts present deviations lower than ±2.5 (showed as circles). This represents an error of 0.01 g/cm³ in a 4 m solution. Some salts of lithium, strontium, calcium, and barium exhibit larger deviations between ±2.5 and ±5 (depicted by the triangles) probably due to the small size in the case of lithium and to the divalent character in the rest of cations. There is one salt, BaBr₂, which deviates almost to ±10 contrary to the other barium salts but we do not have an explanation for that.

Finally, we have also considered a three-component mixture containing two salts and water to see if this approach can be also extrapolated to these more complex systems. As presented in Table V, the results obtained for the densities of NaCl + KCl aqueous solutions with different compositions agree well with the experimental ones and with those obtained with the original Madrid-2019(TIP4P/2005) model.

B. Viscosities

Let us address another crucial property of interest in aqueous solutions. We now turn our attention to the calculation of viscosities for the Madrid-2019(TIP4P/Ice) model at various concentrations of NaCl. However, before delving into this discussion, it is pertinent to talk about the viscosities of the TIP4P/Ice and TIP4P/2005 models separately.

For pure water, the viscosity (at room T and p) predicted by using the TIP4P/2005 model closely aligns with the experimental result (0.85 vs 0.89 mPa · s), as demonstrated in a previous study.[143] In contrast, the recent work of Baran et al.[148] reveals that TIP4P/Ice exhibits a significantly higher viscosity (at room T and p) compared to the experimental value. Our calculations for the viscosity of TIP4P/Ice at 298.15 K and 1 bar yield a result of 1.63 mPa · s, compared to the experimental value of 0.89 mPa · s.

Given the distinct viscosities of the water models, it is insightful to examine the difference between the calculated viscosity at a specific salt concentration and the viscosity of the model for pure water. In Fig. 3, we show this viscosity difference as a function of salt concentration. It becomes evident that the change in viscosity of the Madrid-2019(TIP4P/Ice) model (for a certain concentration) surpasses that of the Madrid-2019(TIP4P/2005) model. Consequently, simulating this new model would result in slower dynamics compared to the original Madrid-2019(TIP4P/2005) model.

Nevertheless, it is crucial to note that the Madrid-2019(TIP4P/Ice) model can be used for describing ices, hydrates,

TABLE IV. Comprehensive comparison of Madrid-2019(TIP4P/2005) and Madrid-2019(TIP4P/Ice) models. We show the number of contact ion pairs (CIP), densities, and the difference $\Delta\rho$ [see Eq. (4)] between the densities of the salty solutions for a concentration close to the experimental solubility of each salt and the density of pure water for each model at 1 bar and 298.15 K.

Salt	m	Madrid-2019(TIP4P/2005)			Madrid-2019(TIP4P/Ice)		
		CIP	ρ	$\Delta\rho$	CIP	ρ	$\Delta\rho$
	mol/kg		kg/m^3			kg/m^3	
Water	0	$\cdots$	997.3	0	$\cdots$	993.12	0
NaF	0.9	0.02	1036.4	39.1	0.01	1032.24	39.12
KF	17	1.15	1456.5	459.2	0.86	1455.9	462.78
RbF	28	2.45	2220.9	1223.6	2.15	2229.32	1236.2
CsF	37	3.30	2982.2	1984.9	3.20	2995.83	2002.71
LiCl	12	0.01	1213.0	215.7	0.01	1225.22	232.1
NaCl	6	0.17	1194.6	197.3	0.10	1193.9	200.78
KCl	4.5	0.38	1168.8	171.5	0.27	1165.16	172.04
RbCl	7	0.23	1444.8	447.5	0.18	1442.85	449.73
CsCl	11	0.48	1898.9	901.6	0.40	1901.40	908.28
MgCl$_2$	5	0	1302.3	305.0	0	1292.14	299.02
CaCl$_2$	6	0.02	1371.5	374.2	0.08	1353.48	360.36
SrCl$_2$	3	0.14	1343.5	346.2	0.04	1345.3	352.18
BaCl$_2$	1.5	0.02	1245.7	248.4	0.01	1242.6	249.48
LiBr	20	1.50	1700.9	703.6	1.30	1761.88	768.76
NaBr	8	0.24	1484.2	486.9	0.14	1486.66	493.54
KBr	5	0.29	1337.8	340.5	0.22	1334.13	341.01
RbBr	7	0.58	1628.9	631.6	0.48	1628.76	635.64
CsBr	5	0.37	1641.3	644.0	0.35	1638.68	645.56
MgBr$_2$	5	0	1606.7	609.4	0	1600.19	607.07
CaBr$_2$	7	0.04	1781.5	784.2	0.03	1750.23	757.11
SrBr$_2$	3.5	0.01	1601.09	603.79	0.003	1615.5	622.38
BaBr$_2$	3	0.13	1612.08	614.78	0.06	1640.2	647.08
LiI	12	0.01	1830.8	833.5	0.01	1859.8	866.68
NaI	12	1.12	1920.7	923.4	0.40	1932.74	939.62
KI	8	0.30	1675.2	677.9	0.32	1675.51	682.39
RbI	7	0.60	1785.3	788.0	0.60	1787.25	794.13
CsI	3	0.35	1500.2	502.9	0.32	1496.97	503.85
MgI$_2$	5	0	1865.0	867.7	0	1857.21	864.09
CaI$_2$	7	0	2072.4	1075.1	0	2036.0	1042.88
SrI$_2$	4	0.38	1874.4	877.1	0.16	1888.7	895.58
BaI$_2$	5	0.12	2172.6	1175.3	0.07	2184.12	1191.00
Li$_2$SO$_4$	3	0	1212.1	214.8	0	1209.44	216.32
Na$_2$SO$_4$	1.5	0.37	1162.6	165.3	0.08	1159.52	166.4
K$_2$SO$_4$	0.6	0.88	1074.4	77.1	0.12	1071.23	78.11
Rb$_2$SO$_4$	1.5	0.70	1275.2	277.9	0.21	1272.34	279.22
Cs$_2$SO$_4$	5	1.25	2003.5	1006.2	0.13	2005.32	1012.2
MgSO$_4$	2.5	0	1247.0	249.7	0	1241.92	248.8
NH$_4$F	5	0.7	1063.18	65.88	0.42	1059.41	66.29
NH$_4$Cl	7	0	1075.02	77.72	0	1067.71	74.59
NH$_4$Br	7	0	1271.65	274.35	0	1264.43	271.31
NH$_4$NO$_3$	26	3.8	1314.79	317.49	3.6	1320.97	327.85
LiNO$_3$	14	0	1348.29	350.99	0	1366.94	373.82
NaNO$_3$	10	0.6	1366.16	368.86	0.45	1377.38	384.26
KNO$_3$	4	0.7	1196.18	198.88	0.75	1199.41	206.29
RbNO$_3$	4	2.3	1317.42	320.12	2.25	1319.31	326.19
CsNO$_3$	1	2.3	1129.35	132.05	0.71	1127.71	134.59
Mg(NO$_3$)$_2$	5	0	1393.0	395.7	0	1396.43	403.31
Ca(NO$_3$)$_2$	9	1.1	1601.28	608.16	0.95	1600.00	606.88
Sr(NO$_3$)$_2$	3	1.2	1393.5	396.2	0.64	1398.45	405.33
Ba(NO$_3$)$_2$	0.3	0.06	1057.3	60.0	0.06	1056.35	63.23

FIG. 2. Difference between $\Delta \rho$ [see Eq. (4)] of the Madrid-2019(TIP4P/2005) model and $\Delta \rho$ of the Madrid-2019(TIP4P/Ice) model divided by the studied molality of each salt. When deviations are smaller than ± 2.5, we employ circles. The triangles are for deviations between ± 2.5 and ± 5, and the squares are for deviations larger than ± 5.

FIG. 3. Difference between the viscosity at each concentration and the viscosity of pure water for each model as a function of concentration for aqueous NaCl solutions at 298.15 K and 1 bar. Blue circles: Madrid-2019(TIP4P/2005) force field ($\eta_0 = 0.85$ mPa s). Red squares: Madrid-2019(TIP4P/Ice) force field ($\eta_0 = 1.63$ mPa s). The solid line is a fit of experimental data taken from Refs. 155 and 156.

and solid phases of water in the presence of salt. The melting point of TIP4P/Ice is 270 K (i.e., 20 K higher than that of TIP4P/2005, which is 250 K), and the dynamics are faster at higher temperatures. Therefore, despite the Madrid-2019(TIP4P/Ice) model exhibiting higher viscosities, it would be simulated at higher temperatures (20 K higher) for a certain degree of supercooling, thus yielding similar dynamics than the original Madrid-2019(TIP4P/2005) model. To confirm this fact, we have evaluated the diffusion coefficients of water in pure water and in a 4 m aqueous solution of NaCl using both the TIP4P/Ice and the TIP4P/2005 water at the melting point of each force field. The results are presented in Table VI, and it is shown that the diffusion coefficients of water both in pure water or in 4 m NaCl solutions at 270 K [for Madrid-2019(TIP4P/Ice)] and 250 K [for Madrid-2019(TIP4P/2005)] are similar. In fact,

those of Madrid-2019(TIP4P/Ice) are slightly larger than those of Madrid-2019(TIP4P/2005). It should be noted that diffusion coefficients are affected by finite size effects.[149–154] However, since we only wanted to compare the diffusion between both models at the considered temperatures, we have not applied the Yeh and Hummer corrections,[154] which would have been rather small for our systems (~5000 particles).

C. Structural features

Once the densities and viscosities of the Madrid-2019(TIP4P/Ice) model have been examined, it is interesting to

TABLE V. Densities (in kg/m^3) for ternary solutions at T = 298.15 K and p = 1 bar. Experimental data are from Ref. 147. m_1 and m_2 are the molalities (in mol/kg) of the salts labeled as (1) [NaCl] and (2) [KCl], respectively. $m_{tot} = m_1 + m_2$ is the total concentration.

NaCl (1) + KCl (2) + H$_2$O								
Expt.			Madrid-2019(TIP4P/2005)			Madrid-2019(TIP4P/Ice)		
m_{tot}	m_1/m_2	Density	m_{tot}	m_1/m_2	Density	m_{tot}	m_1/m_2	Density
2.3760	2.9867	1088	2.4	3	1089	2.4	3	1086
3.9943	0.3325	1148	4	1/3	1149	4	1/3	1146

TABLE VI. Diffusion coefficients of water in pure water and in 4 m NaCl aqueous solutions calculated with the Madrid-2019(TIP4P/2005) and the Madrid-2019(TIP4P/Ice) models. The simulations have been carried out at the melting temperature of Ice I$_h$ for each model.

Model	System	T (K)	$D_{H_2O} \times 10^5$ (cm^2 s^{-1})
TIP4P/2005	Water	250	0.39
TIP4P/Ice	Water	270	0.40
Madrid-2019(TIP4P/2005)	4 m NaCl	250	0.19
Madrid-2019(TIP4P/Ice)	4 m NaCl	270	0.22

TABLE VII. Position of the first maximum of the ion–water oxygen RDF for the different ions of the Madrid-2019 model using both the Madrid-2019(TIP4P/2005) and the Madrid-2019(TIP4P/Ice) models. For the polyatomic ions, we have considered the distances between the central atom and the water oxygen.

Ion	Ion–water distance (Å)	
	Madrid-2019 (TIP4P/2005)	Madrid-2019 (TIP4P/Ice)
Li^+	1.84	1.84
Na^+	2.33	2.33
K^+	2.73	2.72
Rb^+	2.75	2.74
Cs^+	2.86	2.84
Mg^{2+}	1.92	1.92
Ca^{2+}	2.38	2.35
Sr^{2+}	2.60	2.60
Ba^{2+}	2.84	2.84
NH_4^+	2.66	2.63
F^-	2.77	2.75
Cl^-	3.05	3.02
Br^-	3.15	3.12
I^-	3.28	3.27
NO_3^-	3.61	3.61
SO_4^{2-}	3.75	3.74

assess whether there have been any alterations of the structural features of the solution. Accordingly, we investigated ion–water oxygen distances using both models: the original Madrid-2019(TIP4P/2005) and the recently developed Madrid-2019(TIP4P/Ice). In Table VII, we have collected the ion–water distances (calculated as the position of the first maximum of the ion–water oxygen RDF). It can be observed that the distances exhibit a minimal variation when comparing the two models. However, the fact that the distances for the Madrid-2019(TIP4P/Ice) model are slightly shorter (less than 1%) than those in the Madrid-2019(TIP4P/2005) model is noteworthy. This can again be explained due to a stronger Coulumbic interaction between the ions and the TIP4P/Ice attributable to the higher partial charges of the water model (compared to those of the TIP4P/2005), which shortens the oxygen–ion distances. This stronger Coulombic interaction would also explain why in Table IV the $\Delta\rho$ values for Madrid-2019(TIP4P/Ice) are somewhat higher than those for Madrid-2019(TIP4P/2005) and, for the same reason, in Fig. 2, most of the deviations presented are negative.

At this point, it is interesting to highlight that the strategy used in this work could probably be extended to other systems, as deep eutectic solvents, ionic liquids, or even proteins. Further work is needed to study this possibility in more detail. It is likely that this approach will work better when the charges (or partial charges) between two different force fields are the same or very similar. This is certainly the case here, as the ion charges are identical and the partial charges of the water models are quite alike.

D. Freezing temperature depression

When salt is added to water, the freezing point of the solution decreases due to a phenomenon known as freezing point depression. In recent years, efforts have been made to address this effect through computer simulations. Kim and Yethiraj were among the pioneers who tackled this issue by employing direct coexistence simulations to study the freezing depression of ice.[144] Subsequently, Conde et al.[145] also conducted direct coexistence simulations using the TIP4P/2005 water model and a unit charge model for ions. More recently, simulations employing the Madrid-2019(TIP4P/2005) model for various salts have been carried out,[124,131] demonstrating the efficacy of the model in describing how the melting point shifts when a salt is added.

However, it might be useful to not only to replicate the experimental shift (i.e., the difference between the freezing point of pure water and the freezing point of the salt solution) but also accurately predict the absolute temperature at which the system freezes. To achieve this, we employ our new proposed combination of the Madrid-2019 model with the TIP4P/Ice force field.

To evaluate the freezing depression, we have followed the methodology proposed by Noya and co-workers.[124] This approach involves bringing two phases (ice and an aqueous electrolyte solution) into contact. According to the phase rule, for a two component system (water and salt, i.e., $C = 2$), under fixed pressure and temperature, the system reaches the equilibrium at a specific concentration of salt in the aqueous solution. This equilibrium is achieved either by melting some ice (resulting in a decrease in NaCl concentration in the aqueous phase from its initial value) or freezing some water (leading to an increase in the NaCl concentration in the aqueous phase from its initial value). In Fig. 4, we have plotted the concentration of the aqueous phase as a function of time. Similarly to our previous study,[120] simulations were performed for a duration of 2 μs, with the equilibrium molality calculated from the average of the last 1 μs. However, for KCl, the simulation was prolonged for 4 μs to ensure the system's equilibration, and the calculated molality represents the average of the last 2 μs. In all cases, it is evident that the molality within the analyzed time range achieves equilibrium, exhibiting fluctuations around an average value.
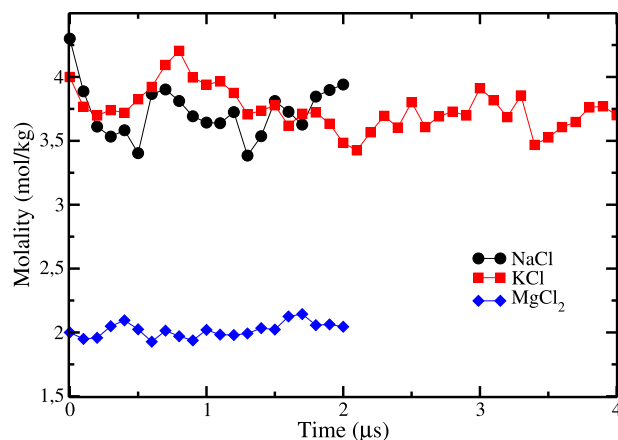
FIG. 4. Molality of the aqueous solution phase as a function of the simulation time for different salts evaluated in this work using the Madrid-2019(TIP4P/Ice) model at 1 bar and 256 K for NaCl and KCl and 1 bar and 253 K for MgCl$_2$. Black circles: results for NaCl. Red squares: results for KCl. Blue diamonds: results for MgCl$_2$.
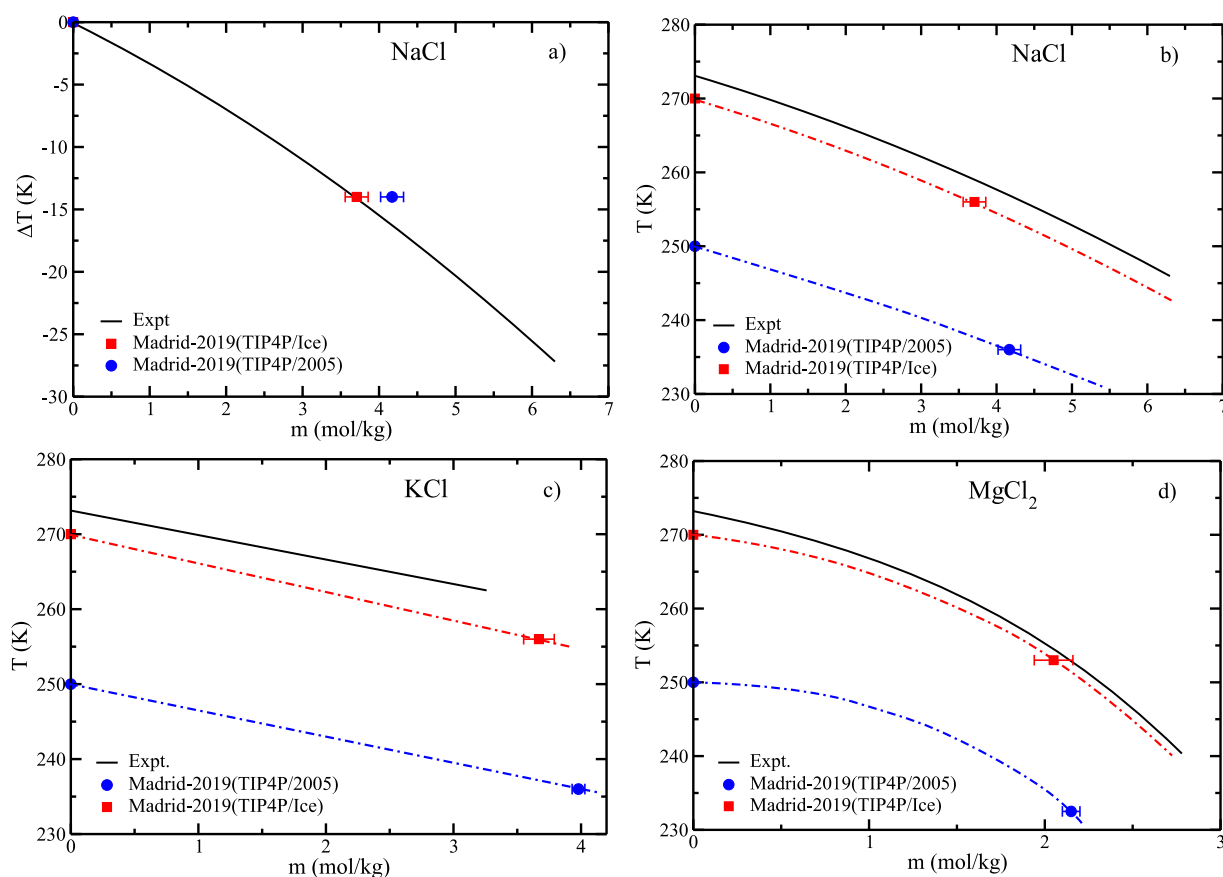
FIG. 5. Freezing point depression (at 1 bar) for the different salt aqueous solutions evaluated in this work. (a) ΔT [i.e., $T_f(m) - T_f(m = 0)$ with $T_f(m = 0)$ being the freezing temperature of ice I_h, 273.15 K from experiments, 270 K for the TIP4P/Ice model, and 250 K for the TIP4P/2005] as a function of concentration of an NaCl solution. (b)–(d) Freezing temperature $T_f(m)$ as a function of concentration for (b) NaCl, (c) KCl, and (d) MgCl$_2$ aqueous solutions. The results using the Madrid-2019(TIP4P/2005) model are represented by the blue circles and are taken from Ref. 120 for NaCl and from Ref. 124 for KCl and MgCl$_2$. The results of this work using the Madrid-2019(TIP4P/Ice) model are represented by the red squares. The continuous black lines are the fit of the experimental data taken from Refs. 157 and 158 for NaCl and from Ref. 159 for KCl and MgCl$_2$. The dashed lines are guide to the eye lines for the simulation results.

After calculating the equilibrium molality at a certain pressure and temperature, we proceed to plot the freezing temperature as a function of concentration for the various studied systems shown in Fig. 5. In previous studies,[120,124] we showed that the shift ΔT in the freezing temperature of water from the aqueous solution $[T_f(m)]$ compared to the freezing temperature of pure water $T_f(m = 0)$ [i.e., $\Delta T = T_f(m) - T_f(m = 0)$] was well described using the Madrid-2019(TIP4P/2005) model. Accordingly, we initially present this ΔT as a function of concentration for both the Madrid-2019(TIP4P/2005) and the Madrid-2019(TIP4P/Ice) water force fields [Fig. 5(a)]. In both cases, the observed shift accurately reproduces the experimental behavior. Nevertheless, the results for the Madrid-2019(TIP4P/Ice) model exhibit an even better agreement with the experimental trend.

However, the primary objective of this work is to accurately replicate the absolute freezing temperature of ice when salt is added.

Consequently, we present the results of the freezing temperature of ice at different concentrations for several salts. This is shown for NaCl in Fig. 5(b). It is clear that the Madrid-2019(TIP4P/2005) model underestimates the absolute values of the freezing temperature of the aqueous solutions due to the original melting point of the employed water model (TIP4P/2005) being 250 K. Nevertheless, the Madrid-2019(TIP4P/Ice) model provides absolute values of the freezing temperature in excellent agreement with the experiments (due, in part, to a correct prediction of the freezing temperature of pure water).

To verify whether this remarkable behavior extends to other systems, we have expanded the study to include two additional salts, KCl and MgCl$_2$. In Figs. 5(c) and 5(d), we present the freezing temperature of water for these salts. In both cases, the Madrid-2019(TIP4P/2005) model underestimates the absolute value of the freezing temperature, as anticipated. However, when combined with

TIP4P/Ice, the results significantly improve, and the freezing temperatures closely align with the experimental values at the studied concentrations. In fact, for the case of $MgCl_2$, the results fall precisely on the experimental line. Thus, we confirm that this combination works effectively for different salts and is not limited to NaCl.

These results are crucial, as they show, for the first time, a freezing depression curve in quasi-quantitative agreement with the experimental data for three different salts, one of them divalent. In fact, since the model presented in this study includes all the ions present in seawater, it would be possible, for the first time, to study the freezing depression of seawater in a quasi-quantitative way. Thus, the Madrid-2019(TIP4P/Ice) model has enormous potential to study, by using computer simulations, the freezing of water from ionic aqueous solutions.

V. CONCLUDING REMARKS

In this work, we have introduced a straightforward strategy to combine the Madrid-2019 force field (originally designed to be used with the TIP4P/2005 model of water) with the TIP4P/Ice model of water. The key idea is to keep ion–ion interactions and the LJ parameters for the ion–water interactions regardless of the water model considered, so that, differences only arise from the water–water interactions and from the Coulombic contribution to the ion–water interaction (due to the small differences in the partial charges of TIP4P/2005 and TIP4P/Ice). Thus, the Madrid-2019(TIP4P/2005) and the Madrid-2019(TIP4P/Ice) models become useful force fields to study ionic solutions. How to choose between these two models? The answer is that one choice could be much better than the other depending on the property under consideration. For instance, to study the maximum in density of water and the impact of salts on it, the Madrid-2019(TIP4P/2005) model should be preferred (as TIP4P/2005 reproduces the experimental value of the TMD of pure water). The same is true when dealing with transport properties of ionic solutions where Madrid-2019(TIP4P/2005) seems more appropriate as again, the TIP4P/2005 describes quite well the transport properties of pure water. However, when dealing with the freezing of water from aqueous ionic solutions or the formation of hydrates from systems containing an ionic solution and a gas, the Madrid-2019(TIP4P/Ice) model is the optimal choice.

In this work, we tested the predictions of the Madrid-2019(TIP4P/Ice) model for several properties and salts. Initially, we observed that the densities do not undergo large changes compared to those of the Madrid-2019(TIP4P/2005) model. Despite the Madrid-2019(TIP4P/Ice) providing reasonably good results for this property, it does not surpass the excellent results of the original Madrid-2019(TIP4P/2005) model.

We then investigated the performance of the model in a transport property of interest: the viscosity. The system exhibited a higher viscosity compared to that of the Madrid-2019(TIP4P/2005) model, as was expected given that the viscosity of the TIP4P/Ice model is almost twice that of the TIP4P/2005 model. Considering that the new model combination is designed for the study of systems such as ices or hydrates, and taking into account the higher melting temperature of TIP4P/Ice, the dynamics of the system are likely similar. Although the model is more viscous (resulting in slower dynamics), it is intended for simulations at higher temperatures (facilitating faster dynamics).

Our subsequent analysis focused on studying the structural features of the model. As we maintained the ion–water interaction, significant changes in the radial distribution functions (RDFs) of cation–water or anion–water were not observed. Only a slight decrease in the distance of cation-O_w or anion-O_w was noted when using the TIP4P/Ice model.

Finally, we investigated the freezing depression and the absolute values of the freezing temperature of ionic aqueous solutions obtaining excellent results compared to experiments. This success demonstrates that the strategy proposed in this work provides excellent results. One can combine a water model using its parameters with an ion force field (utilizing the water–water interactions of the water model and the water–ion interactions of the ion force field) and still obtain reasonably good results while retaining favorable characteristics of both models. This strategy may not work in general, but it works when the two water models are relatively similar in the geometry and in the values of the partial charges (as it is the case of TIP4P/2005 and TIP4P/Ice).

Thus, this work prompts further questions: can we extend this approach to combine any water model with any ion model by simply maintaining the ion–ion and the LJ ion–water interactions? Is this applicable not only to ions but also to more complex systems such as proteins? These interesting questions could be addressed in future works.

SUPPLEMENTARY MATERIAL

In the supplementary material, we provide a Gromacs *topology* file of the Madrid-2019 force field to be used with TIP4P/2005 and another one to be used with TIP4P/Ice.

ACKNOWLEDGMENTS

AUTHOR DECLARATIONS

Conflict of Interest

The authors have no conflicts to disclose.

Author Contributions

Samuel Blazquez: Data curation (equal); Formal analysis (equal); Investigation (equal); Methodology (equal); Writing – original draft (equal); Writing – review & editing (equal). **Lucia F. Sedano**: Data curation (equal); Formal analysis (equal); Investigation (equal); Methodology (equal); Writing – review & editing (equal). **Carlos Vega**: Conceptualization (equal); Funding acquisition (equal); Project administration (equal); Supervision (equal); Writing – review & editing (equal).

DATA AVAILABILITY

The data that support the findings of this study are available within this article.

REFERENCES

[1] R. B. Alley, P. U. Clark, P. Huybrechts, and I. Joughin, Science **310**, 456 (2005).

[2] J. Oerlemans and C. J. Veen, *Ice Sheets and Climate* (Springer, 1984), Vol. 21.

[3] E. D. Sloan and C. A. Koh, *Clathrate Hydrates of Natural Gases*, 3rd ed. (CRC Press, 2007).

[4] J. P. Castillo, H. Rui, D. Basilio, A. Das, B. Roux, R. Latorre, F. Bezanilla, and M. Holmgren, Nat. Commun. **6**, 7622 (2015).

[5] S. Ebashi and M. Endo, Prog. Biophys. Mol. Biol. **18**, 123 (1968).

[6] P. G. Debenedetti, F. Sciortino, and G. H. Zerze, Science **369**, 289 (2020).

[7] L. G. M. Pettersson, R. H. Henchman, and A. Nilsson, Chem. Rev. **116**, 7459 (2016).

[8] P. Gallo, K. Amann-Winkel, C. A. Angell, M. A. Anisimov, F. Caupin, C. Chakravarty, E. Lascaris, T. Loerting, A. Z. Panagiotopoulos, J. Russo *et al.*, Chem. Rev. **116**, 7463 (2016).

[9] E. Sanz, C. Vega, J. Espinosa, R. Caballero-Bernal, J. Abascal, and C. Valeriani, J. Am. Chem. Soc. **135**, 15008 (2013).

[10] P. M. Piaggi, J. Weis, A. Z. Panagiotopoulos, P. G. Debenedetti, and R. Car, Proc. Natl. Acad. Sci. U. S. A. **119**, e227294119 (2022).

[11] M. R. Walsh, C. A. Koh, E. D. Sloan, A. K. Sum, and D. T. Wu, Science **326**, 1095 (2009).

[12] B. C. Knott, V. Molinero, M. F. Doherty, and B. Peters, J. Am. Chem. Soc. **134**, 19544 (2012).

[13] W. L. Jorgensen, J. Chandrasekhar, J. D. Madura, R. W. Impey, and M. L. Klein, J. Chem. Phys. **79**, 926 (1983).

[14] H. J. C. Berendsen, J. R. Grigera, and T. P. Straatsma, J. Phys. Chem. **91**, 6269 (1987).

[15] H. W. Horn, W. C. Swope, J. W. Pitera, J. D. Madura, T. J. Dick, G. L. Hura, and T. Head-Gordon, J. Chem. Phys. **120**, 9665 (2004).

[16] M. Mahoney and W. L. Jorgensen, J. Chem. Phys. **115**, 10758 (2001).

[17] J. L. F. Abascal and C. Vega, J. Chem. Phys. **123**, 234505 (2005).

[18] J. L. F. Abascal, E. Sanz, R. García Fernández, and C. Vega, J. Chem. Phys. **122**, 234511 (2005).

[19] S. Izadi and A. V. Onufriev, J. Chem. Phys. **145**, 074501 (2016).

[20] L.-P. Wang, T. J. Martinez, and V. S. Pande, J. Phys. Chem. Lett. **5**, 1885 (2014).

[21] S. Izadi, R. Anandakrishnan, and A. V. Onufriev, J. Phys. Chem. Lett. **5**, 3863 (2014).

[22] S. Piana, A. G. Donchev, P. Robustelli, and D. E. Shaw, J. Phys. Chem. B **119**, 5113 (2015).

[23] L. F. Sedano, S. Blazquez, and C. Vega, J. Chem. Phys. **161**, 044505 (2024).

[24] H. Jiang, O. A. Moultos, I. G. Economou, and A. Z. Panagiotopoulos, J. Phys. Chem. B **120**, 12358 (2016).

[25] L.-P. Wang, T. Head-Gordon, J. W. Ponder, P. Ren, J. D. Chodera, P. K. Eastman, T. J. Martinez, and V. S. Pande, J. Phys. Chem. B **117**, 9956 (2013).

[26] P. T. Kiss and A. Baranyai, J. Chem. Phys. **138**, 204507 (2013).

[27] V. Babin, C. Leforestier, and F. Paesani, J. Chem. Theory Comput. **9**, 5395 (2013).

[28] S. K. Reddy, S. C. Straight, P. Bajaj, C. Huy Pham, M. Riera, D. R. Moberg, M. A. Morales, C. Knight, A. W. Gotz, and F. Paesani, J. Chem. Phys. **145**, 194504 (2016).

[29] C. Vega and J. L. F. Abascal, Phys. Chem. Chem. Phys. **13**, 19663 (2011).

[30] S. Blazquez and C. Vega, J. Chem. Phys. **156**, 216101 (2022).

[31] C. Vega, J. L. F. Abascal, M. M. Conde, and J. L. Aragones, Faraday Discuss. **141**, 251 (2009).

[32] R. S. Singh, J. W. Biddle, P. G. Debenedetti, and M. A. Anisimov, J. Chem. Phys. **144**, 144504 (2016).

[33] T. Kawasaki and K. Kim, Sci. Adv. **3**, e1700399 (2017).

[34] J. W. Biddle, R. S. Singh, E. M. Sparano, F. Ricci, M. A. González, C. Valeriani, J. L. Abascal, P. G. Debenedetti, M. A. Anisimov, and F. Caupin, J. Chem. Phys. **146**, 034502 (2017).

[35] M. De Marzio, G. Camisasca, M. Rovere, and P. Gallo, J. Chem. Phys. **144**, 074503 (2016).

[36] G. Pallares, M. El Mekki Azouzi, M. A. González, J. L. Aragones, J. L. Abascal, C. Valeriani, and F. Caupin, Proc. Natl. Acad. Sci. U. S. A. **111**, 7936 (2014).

[37] J. L. Aragones, E. G. Noya, J. L. F. Abascal, and C. Vega, J. Chem. Phys. **127**, 154518 (2007).

[38] S. L. Bore, P. M. Piaggi, R. Car, and F. Paesani, J. Chem. Phys. **157**, 054504 (2022).

[39] H. Tanaka, T. Yagasaki, and M. Matsumoto, J. Chem. Phys. **151**, 114501 (2019).

[40] J. M. Miguez, M. M. Conde, J. P. Torre, F. J. Blas, M. M. Pineiro, and C. Vega, J. Chem. Phys. **142**, 124505 (2015).

[41] M. M. Conde and C. Vega, J. Chem. Phys. **133**, 064507 (2010).

[42] M. H. Waage, T. J. Vlugt, and S. Kjelstrup, J. Phys. Chem. B **121**, 7336 (2017).

[43] V. K. Michalis, I. G. Economou, A. K. Stubos, and I. N. Tsimpanogiannis, J. Chem. Phys. **157**, 154501 (2022).

[44] J. Costandy, V. K. Michalis, I. N. Tsimpanogiannis, A. K. Stubos, and I. G. Economou, J. Chem. Phys. **143**, 094506 (2015).

[45] J. Grabowska, S. Blazquez, E. Sanz, I. M. Zerón, J. Algaba, J. M. Míguez, F. J. Blas, and C. Vega, J. Phys. Chem. B **126**, 8553 (2022).

[46] J. Algaba, I. M. Zerón, J. M. Míguez, J. Grabowska, S. Blazquez, E. Sanz, C. Vega, and F. J. Blas, J. Chem. Phys. **158**, 184703 (2023).

[47] Arjun, T. A. Berendsen, and P. G. Bolhuis, Proc. Natl. Acad. Sci. U. S. A. **116**, 19305 (2019).

[48] A. Arjun and P. G. Bolhuis, J. Phys. Chem. B **124**, 8099 (2020).

[49] Z. Zhang, C.-J. Liu, M. R. Walsh, and G.-J. Guo, Phys. Chem. Chem. Phys. **18**, 15602 (2016).

[50] B. Glatz and S. Sarupria, Langmuir **34**, 1190 (2018).

[51] J. Grabowska, S. Blazquez, E. Sanz, E. G. Noya, I. M. Zeron, J. Algaba, J. M. Miguez, F. J. Blas, and C. Vega, J. Chem. Phys. **158**, 114505 (2023).

[52] A. Soni and G. Patey, J. Phys. Chem. C **126**, 6716 (2022).

[53] A. J. Amaya and B. E. Wyslouzil, J. Chem. Phys. **148**, 084501 (2018).

[54] J. R. Espinosa, A. Zaragoza, P. Rosales-Pelaez, C. Navarro, C. Valeriani, C. Vega, and E. Sanz, Phys. Rev. Lett. **117**, 135702 (2016).

[55] J. R. Espinosa, A. L. Diez, C. Vega, C. Valeriani, J. Ramirez, and E. Sanz, Phys. Chem. Chem. Phys. **21**, 5655 (2019).

[56] V. Bianco, P. M. de Hijes, C. P. Lamas, E. Sanz, and C. Vega, Phys. Rev. Lett. **126**, 015704 (2021).

[57] A. Guerra, S. Mathews, J. T. Su, M. Marić, P. Servio, and A. D. Rey, J. Mol. Liq. **379**, 121674 (2023).

[58] J. R. Espinosa, C. Vega, and E. Sanz, J. Phys. Chem. C **122**, 22892 (2018).

[59] H. Niu, Y. I. Yang, and M. Parrinello, Phys. Rev. Lett. **122**, 245501 (2019).

[60] A. Guerra, S. Mathews, M. Marić, P. Servio, and A. D. Rey, Molecules **27**, 5019 (2022).

[61] J. Yan and G. Patey, J. Phys. Chem. A **116**, 7057 (2012).

[62] D. E. Smith and L. X. Dang, J. Chem. Phys. **100**, 3757 (1994).

[63] I. S. Joung and T. E. Cheatham, J. Phys. Chem. B **112**, 9020 (2008).

[64] W. R. Smith, I. Nezbeda, J. Kolafa, and F. Moučka, Fluid Phase Equilib. **466**, 19 (2018).

[65] J. Chandrasekhar, D. C. Spellmeyer, and W. L. Jorgensen, J. Am. Chem. Soc. **106**, 903 (1984).

[66] T. Straatsma and H. Berendsen, J. Chem. Phys. **89**, 5876 (1988).

[67] J. Aqvist, J. Phys. Chem. **94**, 8021 (1990).

[68] L. X. Dang, J. Chem. Phys. **96**, 6970 (1992).

[69] D. Beglov and B. Roux, J. Chem. Phys. **100**, 9050 (1994).

[70] B. Roux, Biophys. J. **71**, 3177 (1996).

[71] Z. Peng, C. S. Ewig, M.-J. Hwang, M. Waldman, and A. T. Hagler, J. Phys. Chem. A **101**, 7243 (1997).

[72] S. Weerasinghe and P. E. Smith, J. Chem. Phys. **119**, 11342 (2003).

[73] K. P. Jensen and W. L. Jorgensen, J. Chem. Theory Comput. **2**, 1499 (2006).

[74] G. Lamoureux and B. Roux, J. Phys. Chem. B **110**, 3308 (2006).

25 August 2025 10:04:49

[75] J. Alejandre and J.-P. Hansen, Phys. Rev. E **76**, 061505 (2007).

[76] P. J. Lenart, A. Jusufi, and A. Z. Panagiotopoulos, J. Chem. Phys. **126**, 044509 (2007).

[77] D. Corradini, M. Rovere, and P. Gallo, J. Chem. Phys. **132**, 134508 (2010).

[78] K. M. Callahan, N. N. Casillas-Ituarte, M. Roeselová, H. C. Allen, and D. J. Tobias, J. Phys. Chem. A **114**, 5141 (2010).

[79] H. Yu, T. W. Whitfield, E. Harder, G. Lamoureux, I. Vorobyov, V. M. Anisimov, A. D. MacKerell, Jr., and B. Roux, J. Chem. Theory Comput. **6**, 774 (2010).

[80] M. M. Reif and P. H. Hünenberger, J. Chem. Phys. **134**, 144104 (2011).

[81] M. B. Gee, N. R. Cox, Y. Jiao, N. Bentenitis, S. Weerasinghe, and P. E. Smith, J. Chem. Theory Comput. **7**, 1369 (2011).

[82] S. Deublein, J. Vrabec, and H. Hasse, J. Chem. Phys. **136**, 084501 (2012).

[83] A. H. Mao and R. V. Pappu, J. Chem. Phys. **137**, 064104 (2012).

[84] S. Mamatkulov, M. Fyta, and R. R. Netz, J. Chem. Phys. **138**, 024505 (2013).

[85] F. Moučka, I. Nezbeda, and W. R. Smith, J. Chem. Theory Comput. **9**, 5076 (2013).

[86] P. T. Kiss and A. Baranyai, J. Chem. Phys. **141**, 114501 (2014).

[87] J. Kolafa, J. Chem. Phys. **145**, 204509 (2016).

[88] R. Elfgen, M. Hülsmann, A. Krämer, T. Köddermann, K. N. Kirschner, and D. Reith, Eur. Phys. J.: Spec. Top. **225**, 1391 (2016).

[89] I. Pethes, J. Mol. Liq. **242**, 845 (2017).

[90] T. Yagasaki, M. Matsumoto, and H. Tanaka, J. Chem. Theory Comput. **16**, 2460 (2020).

[91] S. Blazquez, M. M. Conde, J. L. F. Abascal, and C. Vega, J. Chem. Phys. **156**, 044505 (2022).

[92] M. Kohagen, P. E. Mason, and P. Jungwirth, J. Phys. Chem. B **120**, 1454 (2015).

[93] C. Vega, Mol. Phys. **113**, 1145 (2015).

[94] I. V. Leontyev and A. A. Stuchebrukhov, J. Chem. Phys. **130**, 02B609 (2009).

[95] I. V. Leontyev and A. A. Stuchebrukhov, J. Chem. Theory Comput. **6**, 3153 (2010).

[96] I. V. Leontyev and A. A. Stuchebrukhov, J. Chem. Theory Comput. **6**, 1498 (2010).

[97] I. V. Leontyev and A. A. Stuchebrukhov, Phys. Chem. Chem. Phys. **13**, 2613 (2011).

[98] I. V. Leontyev and A. A. Stuchebrukhov, J. Chem. Theory Comput. **8**, 3207 (2012).

[99] I. V. Leontyev and A. A. Stuchebrukhov, J. Chem. Phys. **141**, 014103 (2014).

[100] Z. Kann and J. Skinner, J. Chem. Phys. **141**, 104507 (2014).

[101] E. Pluhařová, P. E. Mason, and P. Jungwirth, J. Phys. Chem. A **117**, 11766 (2013).

[102] M. Kohagen, P. E. Mason, and P. Jungwirth, J. Phys. Chem. B **118**, 7902 (2014).

[103] E. Duboué-Dijon, P. E. Mason, H. E. Fischer, and P. Jungwirth, J. Phys. Chem. B **122**, 3296 (2017).

[104] T. Martinek, E. Duboué-Dijon, Š. Timr, P. E. Mason, K. Baxová, H. E. Fischer, B. Schmidt, E. Pluhařová, and P. Jungwirth, J. Chem. Phys. **148**, 222813 (2018).

[105] R. Fuentes-Azcatl and M. C. Barbosa, J. Phys. Chem. B **120**, 2460 (2016).

[106] R. Fuentes-Azcatl and M. C. Barbosa, Physica A **491**, 480 (2018).

[107] J. Li and F. Wang, J. Chem. Phys. **143**, 194505 (2015).

[108] E. E. Bruce and N. F. A. van der Vegt, J. Chem. Phys. **148**, 222816 (2018).

[109] M. Soniat and S. W. Rick, J. Chem. Phys. **137**, 044511 (2012).

[110] A. J. Lee and S. W. Rick, J. Chem. Phys. **134**, 184507 (2011).

[111] M. Soniat and S. W. Rick, J. Chem. Phys. **140**, 184703 (2014).

[112] M. Soniat, G. Pool, L. Franklin, and S. W. Rick, Fluid Phase Equilib. **407**, 31 (2016).

[113] Y. Yao, M. L. Berkowitz, and Y. Kanai, J. Chem. Phys. **143**, 241101 (2015).

[114] J. Dockal, M. Lisal, and F. Moucka, J. Mol. Liq. **362**, 119659 (2022).

[115] P. Habibi, A. Rahbari, S. Blazquez, C. Vega, P. Dey, T. J. Vlugt, and O. A. Moultos, J. Phys. Chem. B **126**, 9376 (2022).

[116] P. Habibi, J. R. Postma, J. T. Padding, P. Dey, T. J. Vlugt, and O. A. Moultos, Ind. Eng. Chem. Res. **62**, 11992 (2023).

[117] I. M. Zeron, J. L. F. Abascal, and C. Vega, J. Chem. Phys. **151**, 134504 (2019).

[118] V. M. Trejos, M. de Lucas, C. Vega, S. Blazquez, and F. Gamez, J. Chem. Phys. **159**, 224501 (2023).

[119] S. Blazquez, I. C. Bourg, and C. Vega, J. Chem. Phys. **160**, 046101 (2024).

[120] S. Blazquez, M. M. Conde, and C. Vega, J. Chem. Phys. **158**, 054505 (2023).

[121] S. Blazquez, J. Abascal, J. Lagerweij, P. Habibi, P. Dey, T. J. H. Vlugt, O. A. Moultos, and C. Vega, J. Chem. Theory Comput. **19**, 5380 (2023).

[122] S. Blazquez, I. M. Zeron, M. M. Conde, J. L. F. Abascal, and C. Vega, Fluid Phase Equilib. **513**, 112548 (2020).

[123] S. Blazquez, C. Vega, and M. Conde, J. Mol. Liq. **383**(1), 122031 (2023).

[124] C. P. Lamas, C. Vega, and E. G. Noya, J. Chem. Phys. **156**, 134503 (2022).

[125] E. Duboue-Dijon, M. Javanainen, P. Delcroix, P. Jungwirth, and H. Martinez-Seara, J. Chem. Phys. **153**, 050901 (2020).

[126] B. J. Kirby and P. Jungwirth, J. Phys. Chem. Lett. **10**, 7531 (2019).

[127] L. F. Sedano, S. Blazquez, E. G. Noya, C. Vega, and J. Troncoso, J. Chem. Phys. **156**, 154502 (2022).

[128] F. Gámez, L. F. Sedano, S. Blazquez, J. Troncoso, and C. Vega, J. Mol. Liq. **377**(1), 121433 (2023).

[129] G. Le Breton and L. Joly, J. Chem. Phys. **152**, 241102 (2020).

[130] L. Perin and P. Gallo, J. Phys. Chem. B **127**, 4613 (2023).

[131] L. Yan, D. Scott, and G. Balasubramanian, J. Mol. Liq. **390**, 123198 (2023).

[132] M. F. Dopke, O. A. Moultos, and R. Hartkamp, J. Chem. Phys. **152**, 024501 (2020).

[133] D. van der Spoel, E. Lindahl, B. Hess, G. Groenhof, A. E. Mark, and H. J. C. Berendsen, J. Comput. Chem. **26**, 1701 (2005).

[134] B. Hess, C. Kutzner, D. van der Spoel, and E. Lindahl, J. Chem. Theory Comput. **4**, 435 (2008).

[135] D. Beeman, J. Comput. Phys. **20**, 130 (1976).

[136] S. Nosé, Mol. Phys. **52**, 255 (1984).

[137] W. G. Hoover, Phys. Rev. A **31**, 1695 (1985).

[138] M. Parrinello and A. Rahman, J. Appl. Phys. **52**, 7182 (1981).

[139] U. Essmann, L. Perera, M. L. Berkowitz, T. Darden, H. Lee, and L. G. Pedersen, J. Chem. Phys. **103**, 8577 (1995).

[140] B. Hess, H. Bekker, H. J. C. Berendsen, and J. G. E. M. Fraaije, J. Comput. Chem. **18**, 1463 (1997).

[141] B. Hess, J. Chem. Theory Comput. **4**, 116 (2008).

[142] J. P. Ryckaert, G. Ciccotti, and H. J. C. Berendsen, J. Comput. Phys. **23**, 327 (1977).

[143] M. A. González and J. L. F. Abascal, J. Chem. Phys. **132**, 096101 (2010).

[144] J. S. Kim and A. Yethiraj, J. Chem. Phys. **129**, 124504 (2008).

[145] M. M. Conde, M. Rovere, and P. Gallo, J. Mol. Liq. **261**, 513 (2018).

[146] M. Laliberte and W. E. Cooper, J. Chem. Eng. Data **49**, 1141 (2004).

[147] H.-L. Zhang and S.-J. Han, J. Chem. Eng. Data **41**, 516 (1996).

[148] Ł. Baran, W. Rżysko, and L. G. MacDowell, J. Chem. Phys. **158**, 064503 (2023).

[149] A. T. Celebi, S. H. Jamali, A. Bardow, T. J. H. Vlugt, and O. A. Moultos, Mol. Simul. **47**, 831 (2021).

[150] S. H. Jamali, R. Hartkamp, C. Bardas, J. Sohl, T. J. H. Vlugt, and O. A. Moultos, J. Chem. Theory Comput. **14**, 5959 (2018).

[151] O. A. Moultos, Y. Zhang, I. N. Tsimpanogiannis, I. G. Economou, and E. J. Maginn, J. Chem. Phys. **145**, 074109 (2016).

[152] S. H. Jamali, L. Wolff, T. M. Becker, A. Bardow, T. J. Vlugt, and O. A. Moultos, J. Chem. Theory Comput. **14**, 2667 (2018).

[153] S. H. Jamali, A. Bardow, T. J. Vlugt, and O. A. Moultos, J. Chem. Theory Comput. **16**, 3799 (2020).

[154] I. C. Yeh and G. Hummer, J. Phys. Chem. B **108**, 15873 (2004).

[155] M. Laliberté, J. Chem. Eng. Data **52**, 321 (2007).

[156] M. Laliberte, J. Chem. Eng. Data **52**, 1507 (2007).

[157] H. Haghighi, A. Chapoy, and B. Tohidi, Ind. Eng. Chem. Res. **47**, 3983 (2008).

[158] D. L. Hall, S. M. Sterner, and R. J. Bodnar, Econ. Geol. **83**, 197 (1988).

[159] D. Li, D. Zeng, X. Yin, L. Han, L. Guo, and Y. Yao, Calphad **53**, 78 (2016).